Emission Characteristics and Performance Comparison of Organic Lasers with One-Dimensional Distributed Feedback

2009 Jpn. J. Appl. Phys. 48 052101

(http://iopscience.iop.org/1347-4065/48/5R/052101)

Emission Characteristics and Performance Comparison of Organic Lasers with One-Dimensional Distributed Feedback

Ying Dong[1,2], Han Zhao[1], Junfeng Song[1], FuBin Gao[1], Chuanhui Cheng[3], Yuchun Chang[1], Guotong Du[3], Xuefen Chi[2], Mingbin Yu[4], and Guoqiang Lo[4]

[1] *State Key Laboratory on Integrated Optoelectronics, College of Electronic Science and Engineering, Jilin University, Qianjin Street 2699, Changchun 130012, China*
[2] *College of Communication Engineering, Jilin University, Renmen Street 142, Changchun 130022, China*
[3] *College of Physics and Optoelectronics Technology, Dalian University of Technology, Dalian 116023, China*
[4] *Institute of Microelectronics, A* STAR, 11 Science Park Road, Science Park II, 117685, Singapore*

Received May 12, 2008; revised October 1, 2008; accepted December 6, 2008; published online May 20, 2009

This paper presents optically pumped solid-state organic lasers based on tris(8-hydroxyquinoline) aluminum (Alq_3) doped with the laser dye 4-(dicyanomethylene)-2-*t*-butyl-6(1,1,7,7-tetramethyljulolidy 1-9-enyl)-4*H*-pyran (DCJTB, 2 wt %) using resonator which offers one dimensional distributed feedback. The lasers have been fabricated by deposition of organic films on top of suitable grating microstructures etched into SiN layer. The devices operating in the red spectral region are highly efficient and exhibit low threshold for oscillation (0.3 kW/cm^2). The operating characteristics of the lasers are investigated in detail. The laser oscillation is obtained by optimizing the organic film thickness. The ratio of slot width to grating period is another important parameter to decrease the lasing threshold.

DOI: 10.1143/JJAP.48.052101

1. Introduction

Semiconducting polymers and small molecules organic are promising materials for applications in optoelectronic devices, including light-emitting diodes, photodectectors, full-color displays, and field-effect transistors. In addition, they present excellent characteristics for solid-state lasers by virtue of their high photoluminescence efficiency, low threshold and broad emission spectral range. Lasing in optically pumped organic gain media has been demonstrated for the full visible range[1] and near ultraviolet.[2,3] Distributed feedback (DFB) lasers based on small molecules organic or polymers have also been under investigation.[1–4] DFB lasers exhibit excellent optical mode confinement and low lasing threshold.[5,6] For future electrically pumped organic lasers, reduction in the organic laser thresholds is of crucial importance.

Many organic DFB lasers reported were etched into silica substrate, and their feedback relied on the index contrast between the silica and the organic gain material deposited on top of the grating.[4,7,8] But the index contrast can only be as small as ~0.3. Therefore, many researchers created photonic crystal directly in the organic material, for example by soft lithography.[9,10] The index contrast in this case can only increase by ~0.3, which makes the the index difference about 0.6. In this case, the mode in the structure will be decreased to the silica substrate and be away from the corrugated layer, since silica has a higher index than air. In order to solve this problem, Harbers designed another device structure with a thin layer of a material with higher refractive index.[11] The device was created by depositing the high-index layer (TiO_2) onto the quartz substrate and etching a periodic pattern of holes into the layer. The optical mode was attracted by the corrugated high-index layer, leading to a significant enhancement of the mode coupling. The investigated devices were second-order devices, in which the second-order Bragg mode was propagated in plane and the first-order Bragg mode was scattered out perpendicularly to the plane.

2. Structure of the One-Dimensional Photonic Crystal DFB Lasers

In this work we investigate one-dimensional (1D) DFB surface-emitting lasers consisting of silica substrate, a high index SiN grating layer and organic layer, as shown in Fig. 1(a). These 1D DFB lasers which use thin evaporated films of the organic semiconductor tris(8-hydroxyquinoline) aluminum (Alq_3) doped with the laser dye 4-(dicyanomethylene)-2-*t*-butyl-6(1,1,7,7-tetramethyljulolidy 1-9-enyl)-4*H*-pyran (DCJTB, 2 wt %) as the active gain medium. The lasers exhibit single-mode emission at ~690 nm, with a linewidth of 0.5 nm [full width at half maximum (FWHM)] and a pump threshold of 0.4 kW/cm^2. The lasing threshold of this device is much lower than that of the photonic crystal based organic lasers.[12]

A schematic cross-sectional view of the investigated organic 1D DFB lasers is shown in Fig. 1(a). The thickness of the silica layer in this organic PCDFB laser is 2 µm. The silica is transparent, features low optical losses, and has a low refractive index. The thickness of the SiN layer is 270 nm, the 1D surface relief pattern is formed in SiN by photolithographically. Each pattern is 1.99×1.99 mm^2 on chip. The top view scanning electron microscope (SEM) is measured with JEOL JSM-6700F. The top view SEM of a part of one pattern is shown in Fig. 1(b) in which slot width is only 100 nm, another pattern SEM is shown in Fig. 1(c) in which slot width is 140 nm. In Fig. 1(b), the sample is assigned as laser A; in Fig. 1(c), the sample is assigned as laser B. The grating period of the two samples is 380 nm. Because r/a is an important parameter in photonic crystal, using the analogous method we calculated the ratio of slot width to grating period, the ratio of the laser A is only 0.263 and the laser B is 0.368.

The gain medium Alq_3 and DCJTB (2 wt %) is deposited in vacuum ($<1.0 \times 10^{-3}$ Pa) via thermal evaporation. The thickness of organic is in the range of 270–400 nm. The refractive index of SiN is ~2.2 at a wavelength of 690 nm and that of the organic material is ~1.78. Because SiN exhibits a higher refractive index than the surrounding air-substrate, thus the device can be considered as a silica–SiN–

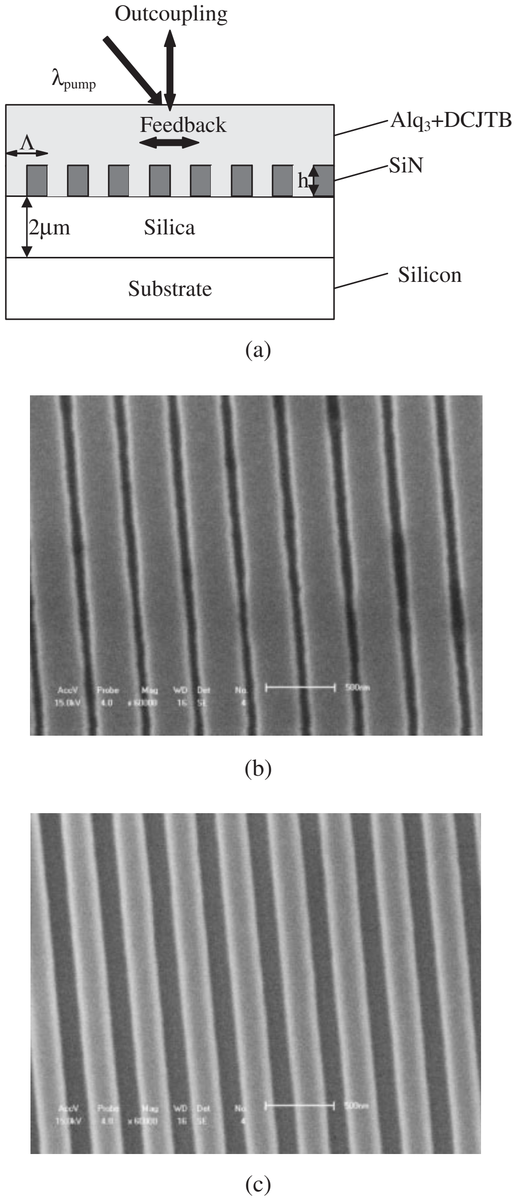

Fig. 1. (a) Schematic cross-sectional view of an investigated second grating, which consist of a second-order sections providing feedback for vertical outcoupling. (b) SEM picture of an investigated second grating with grating period $\Lambda_1 = 380$ nm and slot width = 100 nm. (c) SEM picture of an investigated second grating with grating period $\Lambda_2 = 380$ nm and slot width = 140 nm.

organic (Alq_3 and DCJTB)–air four layers asymmetric planar waveguide. The advantage of inserting SiN layer is that the effective index of the laser mode is raised. Therefore more tightly confinement is achieved by the SiN layer and the organic material in the waveguide. The parameters of the DFB laser are designed to achieve the desired emission wavelength of ~690 nm and FWHM of 0.5 nm. The lasing oscillation occurs near the Bragg resonant wavelength, which is determined from the equation:

$$m\lambda_{\mathrm{Bragg}} = 2n_{\mathrm{eff}}\Lambda,$$

where m indicates the order of diffraction, n_{eff} is the effective refractive index of the propagating mode, and Λ is the grating period. According to this expression, the periodic structure of the 1D DFB laser is second order, which results in a vertical emitting component.

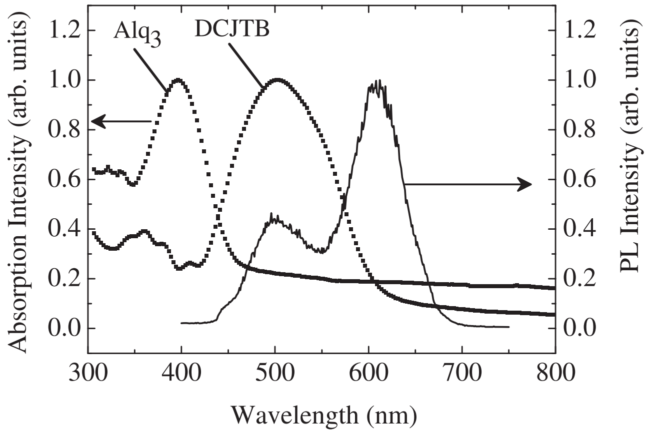

Fig. 2. UV–vis absorption spectra of neat Alq_3 and DCJTB thin film (left curves) and PL spectrum of neat Alq_3 and DCJTB (2 wt %) film (right curve).

3. Laser Oscillation of Organic Photonic Crystal DFB Laser

The absorption spectra of Alq_3 and DCJTB neat thin films are shown respectively in Fig. 2 (left curves), which agree well with the values reported in literatures.[13,14] The absorption spectra are measured by an ultraviolet–visible (UV–vis) spectrometer Shimadzu UV-1700. The absorption spectrum of Alq_3 neat film features maximal at 396 nm and DCJTB thin film features maximal at 503 nm. There are absorptions of Alq_3 and DCJTB at 325 nm. The clean film photoluminescence (PL) spectrum of Alq_3 and DCJTB (2 wt %) in Fig. 2 (right curve) features maximal at 612 nm and another small peak at 496 nm. The small peak shows Alq_3 is excited by the continuous wave He–Cd laser at 325 nm and has the photoluminescence spectrum at 496 nm. During efficient Forster energy transfer from Alq_3 to DCJTB, DCJTB was excited and exhibits a peak at 612 nm. The doping of Alq_3 dopant should effectively improve the lasing actions of DCJTB. The gain material has an index of ~1.78 at this wavelength.

The laser structure is optically pumped with a continuous wave He–Cd laser operating at 325 nm at room temperature in air. The pump beam is incident upon the structures at $\approx 20°$ to the surface normal. A quartz convex lens with $f = 50$ mm focal length is employed to focus the pump laser to a roughly elliptical spot with a diameter 60 μm. The observed laser emission is normal to the surface of the device. Figure 3 shows typical, peak intensity normalized, emission spectra detected in a direction normal to the substrate plane for the 1D DFB laser ($\Lambda = 380$ nm, organic layer thickness ≈ 320 nm) above the lasing threshold (pump energy $= 1.03\,\mathrm{kW/cm^2}$).

4. Results and Discussion

We can readily select the lasing wavelength for our DFB lasers by altering the organic film thickness (hence the effective index of the waveguide). Figure 4 shows the resulting emission spectra by altering the organic film thickness. For the 694.1, 692.2, 688.1, and 686.1 nm lasers, grating period is $\Lambda = 380$ nm, the ratio of slot width to grating period is only 0.263 and organic thickness of ~270, 300, 350, and 400 nm respectively. Here, by adjusting the

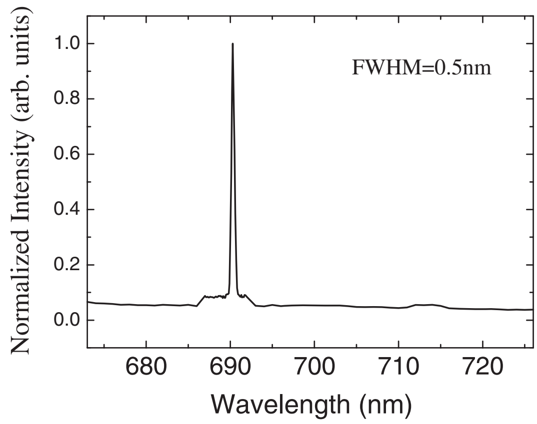

Fig. 3. 1D DFB laser spectrum. The measured FWHM is 0.5 nm. The inset shows peak output intensity from the DFB laser as a function of the excitation energy.

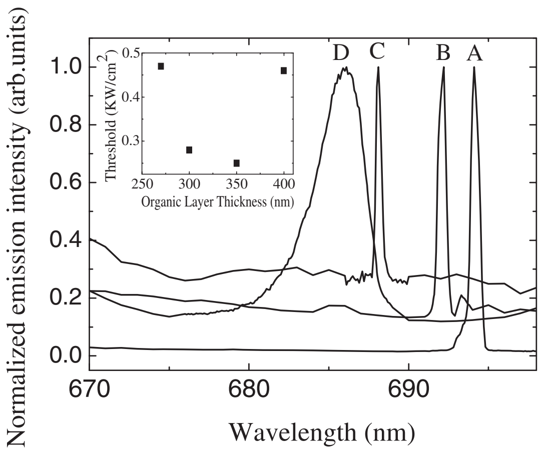

Fig. 4. Broadband tuning of the emission spectra of the 1D DFB lasers. Lasers A–D have grating period Λ = 380 nm, the ratio of slot width to grating period is only 0.263 and organic thickness of ~270, 300, 350, and 400 nm respectively. Top inset: Oscillation threshold as a function of the corresponding organic film thickness.

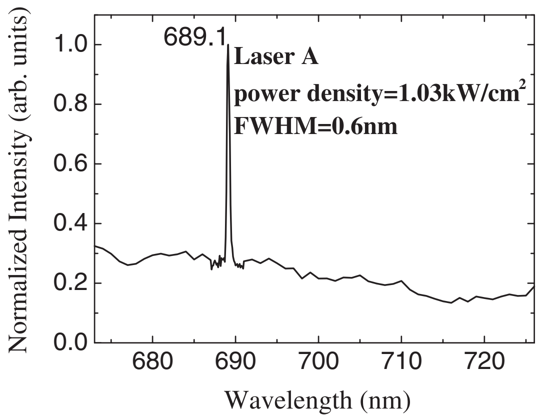

(a)

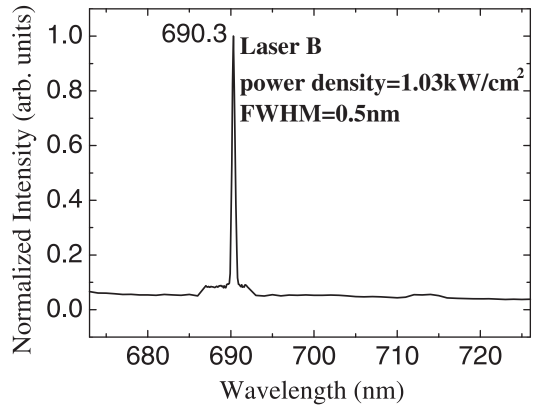

(b)

Fig. 5. Emission spectra of the 1D DFB lasers above their respective thresholds which organic layers are all 320 nm. (a) 1D DFB laser A and (b) 1D DFB laser B emission spectra.

parameter, we tune the 1D DFB laser emission across a spectral range $\Delta\lambda = 8$ nm. The variation of the film thickness leads to change in the effective refractive index and hence, according to Bragg's equation $m\lambda_{\mathrm{Bragg}} = 2n_{\mathrm{eff}}\Lambda$, to a change in the emission wavelength. The inset shows oscillation threshold as a function of the corresponding organic film thickness. As expected, the pump energy needed for laser oscillation tends to decrease as the laser wavelength move towards to the peak of the gain spectrum. In Alq_3 and DCJTB slab waveguides, the maximum optical gain occurs at $\lambda = 612$ nm. Thicker films can support additional lasing modes that compete with the lowest-order mode, the threshold and FWHM of the laser will increase.

Figure 5 shows the emission spectra of the 1D DFB lasers at the same thickness of the organic layer. A sharp lasing peak is observed at 689.1 nm in laser A and the FWHM is about 0.6 nm. In laser B, the lasing peak is at 690.3 nm and the FWHM is about 0.5 nm. About 1.03 kW/cm^2 power density on the sample surface is achieved in this experiment. The FWHM is limited by the resolution of the spectrometer. We did not observe lasing for areas without grating pattern under the same pumping condition. The emission from the structured site features significant spectral narrowing at the resonance wavelength of the DFB structure.

The measured light density as a function of incident pump power is shown in Fig. 6. In both cases, as expected, the thresholds are clearly observed, there are abrupt changes in the slope of the output versus input curves, followed by linear increase of the output signal, then the excitation energy are further increased. The oscillation threshold is ~0.3 kW/cm^2 for the laser A, while for the laser B it is ~0.4 kW/cm^2. The lasers A and B have the same thickness of organic layer. The ratio of slot width to grating period is also an important parameter for decreasing the DFB laser threshold. Otherwise, film quality, measured by surface roughness and consequent scattering should be considered.

5. Conclusions

We have reported solid-state optically pumped DFB lasers comprising a grating patterned SiN based on silica with Alq_3 and DCJTB as gain medium. These structures operated in the red spectra region (686.1 to 694.1 nm) with different organic layer thickness. The effective refractive index and the lasing threshold are regarded as a function of the corresponding organic layer thickness. Because the high index layer in 1D DFB lasers greatly enhances the mode coupling, the 1D DFB lasers based on high index material

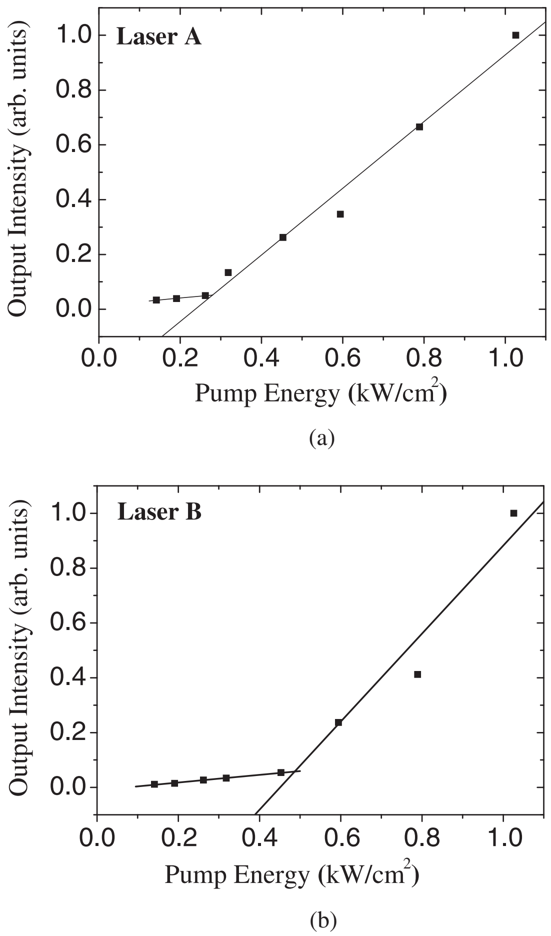

Fig. 6. Plot of the output intensity at the lasing wavelength versus the power energy (*L*–*L* curve).

(SiN) can be significantly small while retaining the same low threshold. The pump energy (lasing threshold) is 0.3 kW/cm^2 when the ratio of slot width to grating period is 0.263, pump energy (lasing threshold) is 0.4 kW/cm^2 when the ratio is 0.368.

Acknowledgments

The authors gratefully acknowledge support by the National Natural Science Foundation of China under Grant Nos. 60576054, 60576043, 60107002, and 60677018, the science and technology development plan of Jilin Province (20080521), Young teacher foundation of DLUT, and Doctoral foundation of DLUT (3005-893327).

1) R. Xia, G. Heliotis, P. N. Stavrinou, and D. D. C. Bradley: Appl. Phys. Lett. **87** (2005) 031104.
2) D. Schneider, T. Rabe, T. Riedl, T. Dobbertin, M. Kroger, E. Becker, H. H. Johannes, W. Kowalsky, T. Weimann, J. Wang, and P. Hinze: Appl. Phys. Lett. **85** (2004) 1886.
3) D. Schneider, T. Rabe, T. Riedl, T. Dobbertin, M. Kroger, E. Becker, H. H. Johannes, W. Kowalsky, T. Weimann, J. Wang, P. Hinze, A. Gerhard, P. Stossel, and H. Vestweber: Adv. Mater. **17** (2005) 31.
4) J. Wang, T. Weimann, P. Hinze, G. Ade, D. Schneider, T. Rabe, T. Riedl, and Y. Kowalsky: Microelectron. Eng. **78** (2005) 364.
5) H. Kogelnik: J. Appl. Phys. **43** (1972) 2327.
6) H. Kogelnik: Appl. Phys. Lett. **18** (1971) 152.
7) C. Karnutsch, C. Gyrtner, V. Haug, U. Lemmer, T. Farrell, B. S. Nehls, U. Scherf, J. Wang, T. Weimann, G. Heliotis, C. Pflumm, J. C. deMello, and D. D. C. Bradley: Appl. Phys. Lett. **89** (2006) 201108.
8) C. Karnutsch, C. Pflumm, G. Heliotis, J. C. Demello, D. D. C. Bradley, J. Wang, T. Weimann, V. Haug, C. Gartner, and U. Lemmer: Appl. Phys. Lett. **90** (2007) 131104.
9) P. Del Carro, A. Camposeo, R. Stabile, E. Mele, L. Persano, R. Cingolani, and D. Pisignano: Appl. Phys. Lett. **89** (2006) 201105.
10) A. Yokoo, H. Suzuki, and M. Notomi: Jpn. J. Appl. Phys. **43** (2004) 4009.
11) R. Harbers, N. Moll, R. F. Mahrt, D. Erni, and W. Bachtold: J. Opt. A **7** (2005) S230.
12) C. Karnutsch, M. Stroisch, M. Punke, U. Lemmer, J. Wang, and T. Weimann: IEEE Photonics Technol. Lett. **19** (2007) 741.
13) W. Lu, H. You, J. F. Fang, and D. G. Ma: Appl. Opt. **46** (2007) 2320.
14) G. Y. Zhong, X. M. Ding, J. Zhou, N. Jiang, W. Huang, and X. Y. Hou: Chem. Phys. Lett. **420** (2006) 347.